Optimal compensation of the Earth's magnetic field while changing the energy at FLASH

DESY summer student program 2009

by

Martin Nuss

TU Graz

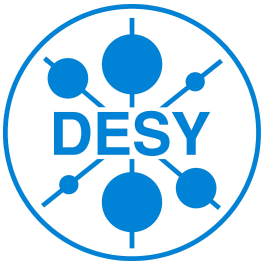

under the supervision of

Dr. Pedro Castro

Machine Physics Group - MPY

DESY, A Research Centre of the Helmholtz Association

summer, 2009

Hamburg, Germany

Contents

1. Introduction

1.1. FLASH

FLASH [1] is a 4^{th} generation synchrotron radiation source based on the SASE principle. It is about $260m$ long and consists of a photo injector as electron source, a superconducting LINAC and a $30m$ long undulator section. This FEL is designed to deliver ultrashort pulses ($\approx 10^{-14}s$) of coherent (monochromatic) radiation tunable from $6.3nm$ to $70nm$ (VUV and soft X-ray) on the GW level.

The main elements of the beamline of FLASH (status August 2009) are shown in figure 1.1. The part of the beamline (starting at $z = 122m$ and ending at $z = 235m$), where the trajectory simulations were done is shown in figure 1.2 in more detail. The scheme of representing the layout of the beamline given in this figure is the same for all plots presented.

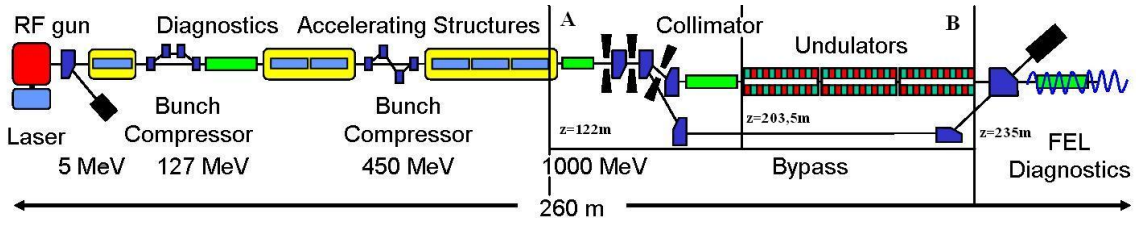

Figure 1.1.: Main elements of the beamline of FLASH (not to scale). The marked area from $z = 122m$ to $z = 235m$ was used for the calculations in this paper and is shown in detail in figure 1.2.

The labeled regions A, and B (shown in figure 1.1) are frequently used within this paper and referred to as "collimator and diagnostics section" (A) which is starting at $z = 122.0m$ and ending at $z = 203.4m$ and "undulator section" (B) which is starting at $z = 203.4m$ and ending at $z = 233.4m$ respectively.

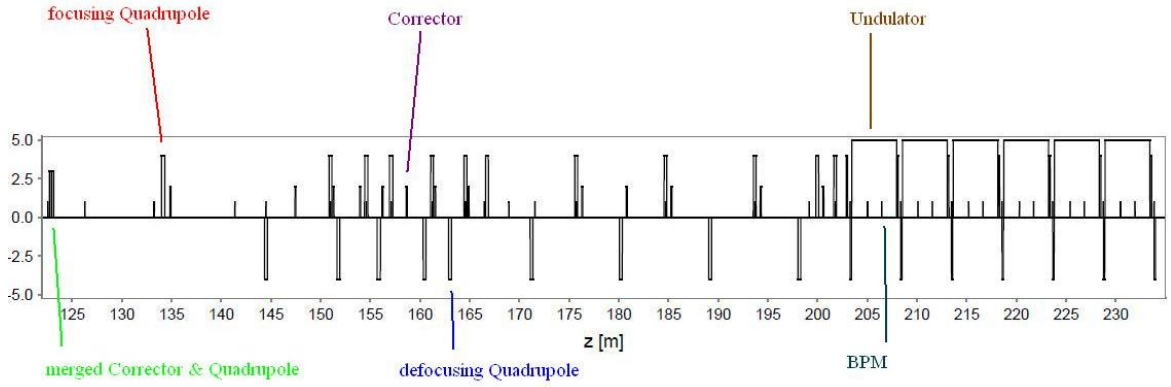

Figure 1.2.: The part of the FLASH beamline (starting at $z = 122m$ and ending at $z = 235m$) which was considered for the calculations in this paper.

1.2. Motivation

Scientists working on synchrotron radiation experiments want to use FLASH at different wavelengths. This is done in FLASH by changing the energy of the electron beam. FLASH is able to operate at an electron beam energy range of about $0.3GeV$ (for $70nm$) to $1.0GeV$ (for $6.3nm$). To achieve a good and stable SASE process it is essential to keep the orbit in the undulator section (almost) unaltered when tuning the energy of the beam. In order to leave the trajectory unaffected while changing the energy, the current of the quadrupoles, correctors and dipoles is rescaled with the relative energy change. The initial current of the quadrupoles $\vec{I}_{q,initial}$ is changed to a new current $\vec{I}_{q,new}$ given by

$$\vec{I}_{q,new} = \frac{E_{new}}{E_{initial}} \vec{I}_{q,initial} \tag{1.1}$$

to keep the quadrupole strength k (defined in chapter 2.2) constant. $E_{initial}$ is the initial energy of the beam and E_{new} is the energy the accelerator is set to. The corrector currents are changed according to

$$\vec{I}_{c,new} = \frac{E_{new}}{E_{initial}} \vec{I}_{c,initial} \tag{1.2}$$

to keep the bending radius ρ (defined in chapter 2.2) constant.
In principle this procedure should result in an unaltered trajectory. However a large change of the trajectory is observed experimentally (see for example [2]).
One contribution for the change of the orbit is due to the Earth's magnetic field. In this paper the effects of the Earth's magnetic field on the trajectory are studied using a simulation program. It is aimed to develop a compensation mechanism using the corrector dipoles.

1.3. Effect of Earth's magnetic field on FLASH

Usually the effects of the Earth's magnetic field are neglected when calculating trajectories for accelerators considering beam energies above $100MeV$. However this paper will show that in case of FLASH the effect of the Earth's magnetic field on the orbit can not be neglected especially when tuning the energy.
The horizontal component of the magnetic field of the Earth does not influence the beam since FLASH is pointing almost in the south-north (see fig. 1.3 left) direction. Thus the Earth's magnetic field and the particle beam in the accelerator are approximately parallel to each other.
In Hamburg however the Earth's magnetic field has a vertical component (see fig. 1.3 right) which was measured to be about $B_{earth} = -30\mu T$ in the FLASH tunnel. This field may cause a deviation of the beam in the unshielded drift spaces which we want to examine.

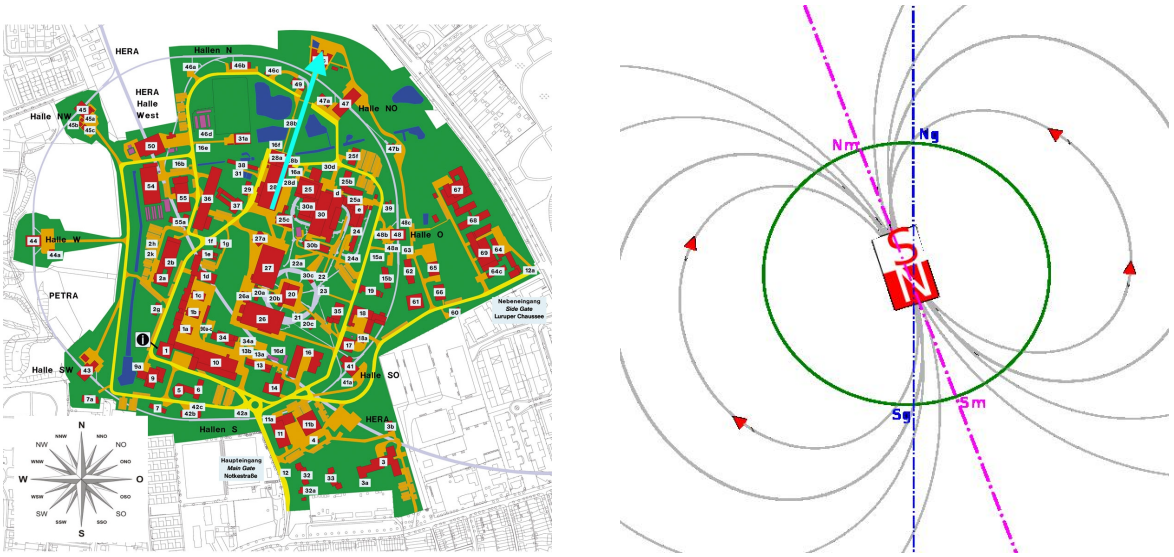

Figure 1.3.: On the left: Map of DESY showing the FLASH facility and its direction pointing almost south-north. On the right: Rough sketch of the magnetic field lines of the Earth. At Hamburg (53°37'59"N/9°58'59"E) the field has a vertical component. (From http://en.wikipedia.org/wiki/Earth's_magnetic_field 23.07.2009)

2. Methods

2.1. Single particle motion in a magnetic field in Lagrangian formalism

To simulate the trajectory we treat the electron beam as a single particle interacting only with electromagnetic fields produced by the elements of the beamline and external fields, neglecting all other interactions in the beamline.

The derivations given in this section follow [3] chapter 1.3 and 2.
We are dealing with the motion of electrons in electromagnetic fields. Since the beam energy of FLASH is in a region of $0.5 - 1.0GeV$ the particles can always be considered as ultra-relativistic (e^- at $E = 0.5GeV$: $v = 0.9995c$). For ultra relativistic electrons the energy E is almost the same as the kinetic energy T, the particle momentum $|p|$ is $\frac{E}{c}$.

The motion of charged particles is governed by the Lorentz force law

$$\vec{F}_L = q(\vec{E} + \vec{v} \times \vec{B}) = m(\gamma \frac{d\vec{v}}{dt} + \gamma^3 \frac{\beta}{c} \frac{d|\vec{v}|}{dt} \vec{v}) \tag{2.1}$$

Using a fully relativistically correct calculation one will arrive at the Lagrangian ($E_\mu \cdot v_\mu$)

$$\mathcal{L}(x, y, z) = -mc^2 \sqrt{1 - \beta^2} + e\vec{A} \cdot \dot{\vec{x}} - e\Phi \tag{2.2}$$

In a second step the curvilinear Frenet-Serret coordinate system is applied. In this special system, the ideal path of the particle is transformed away by applying a local 2D Cartesian coordinate system for the transverse components which moves along the ideal longitudinal path.
The transformation to the new coordinates is

$$\vec{r}(z) = \vec{r}_0(z) + d\vec{r}(z) \quad \text{where } \vec{r}_0(z) \text{ is the reference path} \tag{2.3}$$

$$\vec{u}_x(z) \quad \text{unit vector normal to trajectory (horizontal transverse component)} \tag{2.4}$$

$$\vec{u}_z(z) = \frac{d\vec{r}_0(z)}{dz} \quad \text{unit vector parallel (longitudinal component)} \tag{2.5}$$

$$\vec{u}_y(z) = \vec{u}_z(z) \times \vec{u}_x(z) \quad \text{unit binormal vector (vertical transverse component)} \tag{2.6}$$

The xz plane we call the horizontal and the yz plane the vertical plane.

Introducing the parameter $h = 1 + \kappa_x x + \kappa_y y$, where κ_i are the curvatures of the trajectory, one can rewrite the Lagrangian in the curvilinear system

$$\mathcal{L}(x, y, z) = -mc^2 \sqrt{1 - \frac{1}{c^2}(\dot{x}^2 - \dot{y}^2 - h^2 \dot{z}^2)} + e(\dot{x}A_x + \dot{y}A_y + h\dot{z}A_z) - e\Phi \tag{2.7}$$

In a last step a transformation to (for our application) more practical variables is done changing the independent variable from time t to longitudinal position z (since within each considered element of the beamline the beam energy is constant (i.e. no acceleration takes place)).
The final Lagrangian (without any approximations) is

$$\widetilde{\mathcal{L}}(x, x', y, y', z) = s' + (1 - \delta)\frac{e}{p_0}(x'A_x + y'A_y + hA_{c,z}) - s'\frac{e\Phi}{\gamma m v^2} \tag{2.8}$$

Primed variables are differentiated with respect to z (representing angles instead of velocities). S is the path of the particle ($s = \sqrt{x'^2 + y'^2 + h^2}$), p_0 the ideal momentum and $\delta = \frac{p - p_0}{p_0}$ the deviation

from the ideal momentum.

The resulting set of equations has no analytic solution and even the numerical solution is non trivial. The paraxial approximation ($x' << 1$, $y' << 1$, $s' \approx 1$, $h \approx 1$, $\delta \approx 0$) is applied to the obtained equations of motion. The small terms which are neglected can be reintroduced later doing perturbation theory. The resulting simplified, unperturbed equations of motion are

$$x'' \approx \frac{e}{p_0}(B_y - y'B_z) + \frac{e}{\gamma m v^2}E_x \tag{2.9}$$

$$y'' \approx \frac{e}{p_0}(B_x - x'B_z) + \frac{e}{\gamma m v^2}E_y \tag{2.10}$$

Assuming further the ultra relativistic approximation valid for our purposes ($p_0 \approx E$ and $v \approx c$) we end up with

$$x'' \approx \frac{e}{E}(B_y - y'B_z) \tag{2.11}$$

$$y'' \approx \frac{e}{E}(B_x - x'B_z) \tag{2.12}$$

The obtained linearized equations of motion (eq. 2.12) can now be solved for the case of a quadrupole field with constant gradient along z.
Starting from the equations of motion (eq. 2.12) and inserting the $\vec{B}_{QDP}$ field of a quadrupole magnet

$$V_{QDP} = \frac{E}{ce}\frac{k}{2}(x^2 - y^2) - \frac{E}{ce}kxy \tag{2.13}$$

$$\vec{B}_{QDP} = -\nabla V_{QDP} \tag{2.14}$$

$$\vec{B}_{QDP} = \begin{pmatrix} -\frac{E}{ce}kx + \frac{E}{ce}ky \\ \frac{E}{ce}kx + \frac{E}{ce}ky \\ 0 \end{pmatrix} \tag{2.15}$$

we arrive at

$$x'' - k(x + y) = 0 \tag{2.16}$$

$$y'' + k(x - y) = 0 \tag{2.17}$$

We are now interested in a decoupled one dimensional motion so we set $y = 0$ in the first and $x = 0$ in the second equation yielding the familiar harmonic oscillator equation

$$\xi(z)'' + k\xi(z) = 0 \tag{2.18}$$

where ξ stands for either x or y.
This treatment is possible because in an unrotated quadrupole $F_x \propto B_y = f(x)$ and $F_y \propto B_x = f(y)$. Considering the initial conditions $\xi(0) = \xi_0$ and $\xi'(0) = \xi'_0$ the solution splits into three regions according to k:
For $k = 0$

$$\xi(z) = \xi_0 + z \cdot \xi'_0 \tag{2.19}$$

$$\xi'(z) = \xi'_0 \tag{2.20}$$

For $k > 0$

$$\xi(z) = cos(\sqrt{|k|}z) \cdot \xi_0 + \frac{1}{\sqrt{|k|}}sin(\sqrt{|k|}z) \cdot \xi'_0 \tag{2.21}$$

$$\xi'(z) = -\sqrt{|k|}sin(\sqrt{|k|}z) \cdot \xi_0 + cos(\sqrt{|k|}z) \cdot \xi'_0 \tag{2.22}$$

For $k < 0$

$$\xi(z) = cosh(\sqrt{|k|}z) \cdot \xi_0 + \frac{1}{\sqrt{|k|}} sinh(\sqrt{|k|}z) \cdot \xi_0' \tag{2.23}$$

$$\xi'(z) = \sqrt{|k|} sinh(\sqrt{|k|}z) \cdot \xi_0 + cosh(\sqrt{|k|}z) \cdot \xi_0' \tag{2.24}$$

Putting the resulting equations (eqs. 2.20, 2.22, 2.24) into matrix form one arrives at the transport matrix for a quadrupole which we use in this work to predict the motion of the beam (see next chapter).

2.2. Transport Matrix Formalism

Usually in the approximation of the Hard Edge Model, we can use the transport matrix formalism to describe the trajectory in accelerators or any other device which uses electric and magnetic fields to guide the motion of moving charged particles.
The Hard Edge Model assumes that the contribution to the magnetic field of a specific element is zero outside of it, that is the asymptotically decaying fields and fringe fields are neglected.
This formalism is based on the parameter z, the longitudinal beam coordinate and not on time t, as one would normally expect of dealing with equations of motion.
The main idea of this method is to cut the beamline into parts. It is possible to choose these parts in a way that the magnetic field is constant in each element. Each of these elements can be represented as a single transport matrix. The trajectory at any position of the beamline can be calculated by applying the transport matrix to initial coordinates.
Starting from one initial condition defined by position and angle the trajectory can be calculated within the first element of the beamline. The calculated coordinate at the end of the first element then serves as initial condition for the second element and so on.
A general representation for a one dimensional problem (for example just the horizontal component of the beam) looks like this:

$$\begin{pmatrix} x_{n+1} \\ x'_{n+1} \end{pmatrix} = \begin{pmatrix} R_{11} & R_{12} \\ R_{21} & R_{22} \end{pmatrix} \cdot \begin{pmatrix} x_n \\ x'_n \end{pmatrix} \tag{2.25}$$

The used variables for this one dimensional model are x the horizontal position perpendicular to the beam's longitudinal direction (direction of motion) and x' the angle of the beam.
It is possible to calculate only the trajectory j (different) parts away from the initial position:

$$\begin{pmatrix} x_{n+j} \\ x'_{n+j} \end{pmatrix} = R_j \cdot R_{j-1} \cdot R_{j-2} \cdot ... \cdot R_1 \cdot \begin{pmatrix} x_n \\ x'_n \end{pmatrix} \tag{2.26}$$

Using TMF it is also possible to calculate the coordinates at every point inside the element. For example the matrix to calculate N coordinate points inside a given drift space would look like the following:

$$R_{ds} = \begin{pmatrix} 1 & L/N \\ 0 & 1 \end{pmatrix} \tag{2.27}$$

Attention has to be paid to the fact that it is not possible to superimpose transport matrices. So if two different elements occupy the same space in the beamline one can't just add the matrices. One special example of this situation is discussed below in *E) combined quadrupole - corrector.*

The transport matrices for all elements used in the simulation will now be discussed in more detail.

A) drift space

A field free section of the beamline is called drift space. The trajectory is supposed to be a straight line there, just determined by the trajectory's condition entering the drift space x_0, x'_0 and the drift space's length L.

The transport matrix is easy to get and looks like:

$$R_{ds} = \begin{pmatrix} 1 & L \\ 0 & 1 \end{pmatrix} \tag{2.28}$$

B) drift space modified for external magnetic induction

To be able to investigate the perturbation of the beam due to small external fields, the drift space transport matrices were extended to be able to take static magnetic magnetic fields into account. In addition to the initial beam coordinate and the length of the element the path is now a curve which is also depending on the external magnetic field and the beam energy. These dependencies are accounted for in the parameter ρ, which is the radius of curvature defined by:

$$\rho = \frac{1}{ce}\frac{E}{B} \tag{2.29}$$

$$\rho[m] = \frac{1}{0.299792458}\frac{E[GeV]}{B[T]} \tag{2.30}$$

The transport matrix for such an element is:

$$R_{dsB} = \begin{pmatrix} 1 & L & \frac{1}{2}\frac{L^2}{\rho} \\ 0 & 1 & \frac{L}{\rho} \\ 0 & 0 & 1 \end{pmatrix} \tag{2.31}$$

The extension of the regular 2x2 matrix to a 3x3 matrix is done to be able to deal with constant terms. The calculation of the trajectory now looks like the following.

$$\begin{pmatrix} x_{n+1} \\ x'_{n+1} \\ 1 \end{pmatrix} = \begin{pmatrix} 1 & L & \frac{1}{2}\frac{L^2}{\rho} \\ 0 & 1 & \frac{L}{\rho} \\ 0 & 0 & 1 \end{pmatrix} \cdot \begin{pmatrix} x_n \\ x'_n \\ 1 \end{pmatrix} \tag{2.32}$$

C) corrector dipole

A corrector dipole magnet corrects the beam's direction. It is therefore the same as $R_{ds,B}$ the transport matrix of a drift space with external field. For calculating the bending radius ρ the magnetic field of the corrector is used.

D) quadrupole element

A quadrupole will focus the beam in one direction and defocus it in the other. To obtain an overall focusing a combination of quadrupole lenses is used (focusing-defocusing). For the description of the

properties of the quadrupole the so called quadrupole strength k is used:

$$k = ce\frac{g}{E} \tag{2.33}$$

$$k[\frac{1}{m^2}] = 0.299792458\frac{g[\frac{T}{m}]}{E[GeV]} \tag{2.34}$$

For the equations the parameter ϕ is used, where $\phi = \sqrt{|k|}L$.
The transport matrix for a focusing quadrupole (k>0):

$$R_{qf} = \begin{pmatrix} cos(\phi) & \frac{1}{\sqrt{|k|}}sin(\phi) \\ -\sqrt{|k|}sin(\phi) & cos(\phi) \end{pmatrix} \tag{2.35}$$

The transport matrix for a defocusing quadrupole (k<0):

$$R_{qd} = \begin{pmatrix} cosh(\phi) & \frac{1}{\sqrt{|k|}}sinh(\phi) \\ \sqrt{|k|}sinh(\phi) & cosh(\phi) \end{pmatrix} \tag{2.36}$$

For $k = 0$ the quadrupole is neither focusing nor defocusing but just a drift space without any external field contribution due to the shielding effect arising from the iron yoke.

It is possible to account for the effects of a quadrupole which has an offset x_{offset} from horizontal zero

$$\begin{pmatrix} x_{n+1} \\ x'_{n+1} \end{pmatrix} = R \cdot \begin{pmatrix} x_n - x_{offset} \\ x'_n \end{pmatrix} + \begin{pmatrix} x_{offset} \\ 0 \end{pmatrix} \tag{2.37}$$

E) combined quadrupole - corrector

In some regions of the beamline there is a quadrupole and a corrector placed "on top of each other". As mentioned above one can not add the transport matrices of these two elements in any way to be able to calculate the trajectory there.
Our solution is based on the fact that a quadrupole acts like a dipole (focusing or defocusing) when the beam is off axis. We exploit that fact to virtually shift the horizontal position of the quadrupole by a certain amount to be able to use just the transport matrix for the quadrupole, which then accounts correctly also for the effects of the corrector.
To find the amount the quadrupole has to be shifted in the horizontal axis we take a closer look at the B_y field produced by the quadrupole

$$B_y = g \cdot x \tag{2.38}$$

$$= \underbrace{g \cdot \hat{x}}_{B_y \text{ of Quadrupole}} + \underbrace{g \cdot x_{offset}}_{B_y \text{ of Dipole}} \tag{2.39}$$

where g is the gradient of the magnetic field of the quadrupole.
We split the horizontal distance from the center of the quadrupole in two contributions arising from the orbit itself $\hat{x}$ and a virtual offset x_{offset}. These can now be interpreted again as a contribution of a (unshifted) quadrupole and a dipole (corrector).
Now we examine the B_y field produced by a horizontal corrector

$$B_y = A_0 \cdot I_c \tag{2.40}$$

where A_0 is the field factor of the corrector.
By comparing the vertical magnetic field of the dipole part of the quadrupole and the field of the corrector we can find the x_{offset} the quadrupole has to be shifted by to account for a given corrector

$$B_y = A_0 \cdot I_c = g \cdot x_{offset} \tag{2.41}$$

$$\Rightarrow x_{offset} = \frac{A_0 \cdot I_c}{g} \tag{2.42}$$

F) beam position monitor

A BPM is used to monitor the position of the moving electrons in the beamline, without changing it. Thus there is no transport matrix. The BPMs are mentioned here because they are treated as special points throughout the program to identify the values which can be checked in the control room.

G) undulator

Undulators consist of a series of dipoles and are used to produce synchrotron radiation. In this simulation they are treated as drift spaces without any influence of the external magnetic field. So inside undulators the transport matrix of a drift space R_{ds} is used.

2.3. Dispersion

The dispersion $D(z) = \frac{dx(z)}{\frac{dE}{E_0}}$ is a very useful quantity when studying disturbing effects on a particle beam. In principle the dispersion shows the transverse distribution for a non monochromatic beam. For the single particle calculations done in this paper it may be interpreted as the sensitivity of the trajectory to a change of energy in a given section of the beamline.

According to [2] the dispersion in the undulator section must be smaller than $D = 18mm$ to keep the contribution of the dispersion to the increase of gain length below 10% for all energies at FLASH. The gain length is the distance in which the amount of photons in an undulator is increased by a factor of e. This means a short gain length provides high intensity output over short distances.

3. Program and Comparison with other Simulations

3.1. Program

In order to implement the calculation of the trajectory using TMF (see chapter 2.2) a computer simulation has been written. The technology used for the program called TOP is an object oriented approach in Java using xml input files, JFreeChart as a plotting library, JMinuit as an optimization library and sometimes Matlab to do some comparisons and additional plots, fits and minimizations. For details about the newly developed program itself see [4].

For calculations the following techniques are used within the simulation program:

- The Transport Matrix Formalism (see 2.2)
  TMF is used to calculate the trajectory.

- Different optimization and minimization techniques (see 4.3)
  These different approaches are used to determine the best set of corrector currents to compensate a static external magnetic field.

- Monte Carlo simulation (see 3.3)
  Monte Carlo simulation is used to study the effects of not perfect quadrupole placement on the dispersion relation.

The results of the simulation program TOP have been compared with different existing tools and to experimental data to ensure the quality of our calculations. The agreement is very good in each of the cases.

3.2. Trajectory Comparison

The results of TOP have been compared with the calculated trajectories of an existing and widely used program called MAD-X [5]. The agreement is very good as shown in figure 3.1.

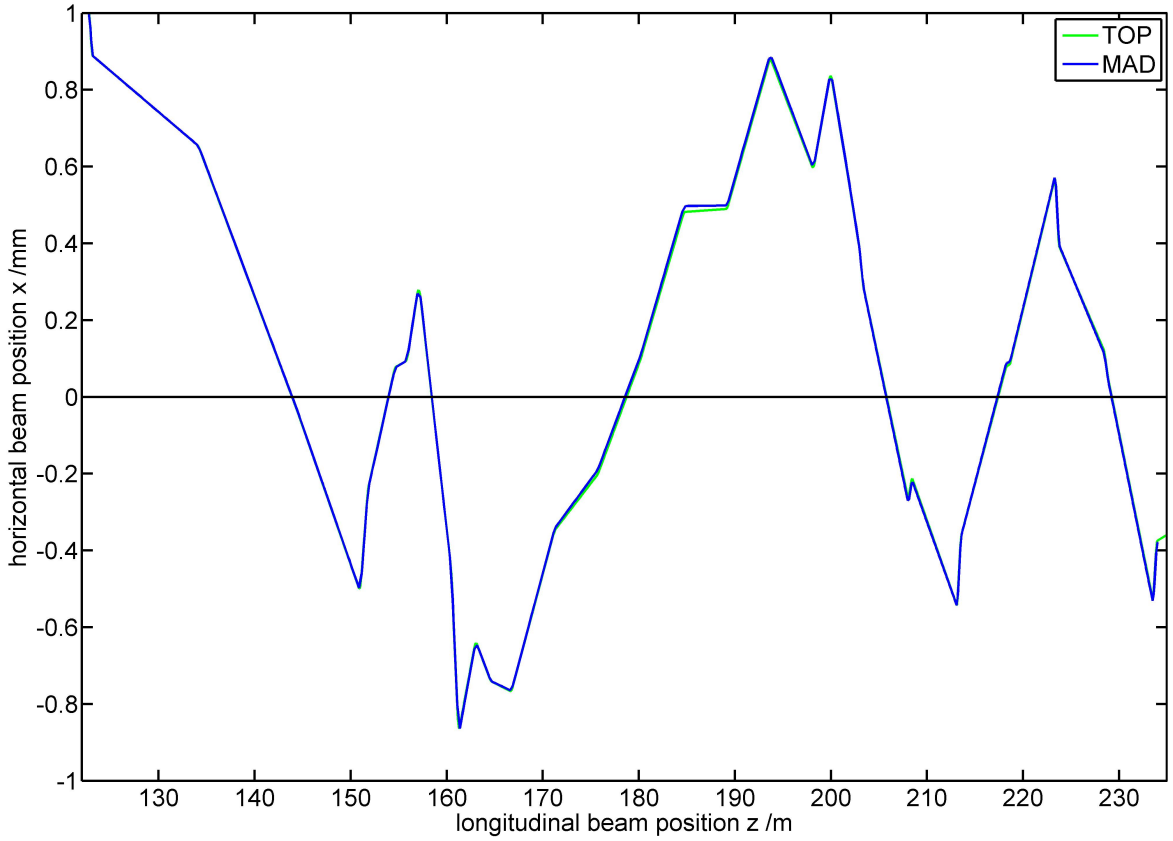

Figure 3.1.: Comparison of trajectories calculated by MAD and TOP for same input parameters

3.3. Dispersion Comparison

We use a Monte Carlo simulation for simulating the effects of misplaced quadrupoles on the dispersion relation. To get an idea of the magnitude of the effect on the dispersion a MCS is done, setting the x offset of all specified quadrupoles in each run (seed) of the simulation to random values within a given standard deviation σ. The preferred mode for generating the random sets of values is a Gaussian distribution centered at $\mu = 0$ with a standard deviation of σ (between $0.1mm$ and $1.0mm$). But it is also possible in the simulation to use uniform distributed random numbers which will then be distributed from $-\sigma$ to $+\sigma$.
For each set of generated random numbers the trajectory and a trajectory which is shifted by $dE_{abs} = 0.0001GeV$ in energy are calculated. Out of these trajectories the dispersion and the characteristic parameters are calculated. After N runs the mean and the standard deviation of all these parameters are obtained.

For our application the MCS was found to yield characteristic parameters which depend linearly on σ as expected. In simulations for different energies it was found that the characteristic parameters do not depend on the beam energy in the MCS. Note that the variable σ denotes not the standard deviation of the result but the standard deviation of the generated random seed numbers and hence the x offset of the quadrupole.

A Monte Carlo simulation done ($N = 100000$ and $\sigma = 0.2mm$ for all quadrupoles) is shown in figure 3.2. It yielded values for the characteristic parameters, which have been calculated for the

undulator section of the beamline. These values are

```
------------------------------------------------------------------------
Results of Monte-Carlo-Simulation for N = 100000 (average values)
------------------------------------------------------------------------
Trajectories:
Integral of x^2/L:          2.640mm
RMS of BPM x positions:     2.507mm
Peak to Peak Trajectory:    9.801mm
Peak to Peak BPM:           7.643mm
------------------------------------------------------------------------
Dispersion:
Integral of D^2/L:         50.426mm
RMS of BPM D positions:    47.909mm
Peak to Peak D:           185.633mm
Peak to Peak D at BPM:    145.661mm
------------------------------------------------------------------------
```

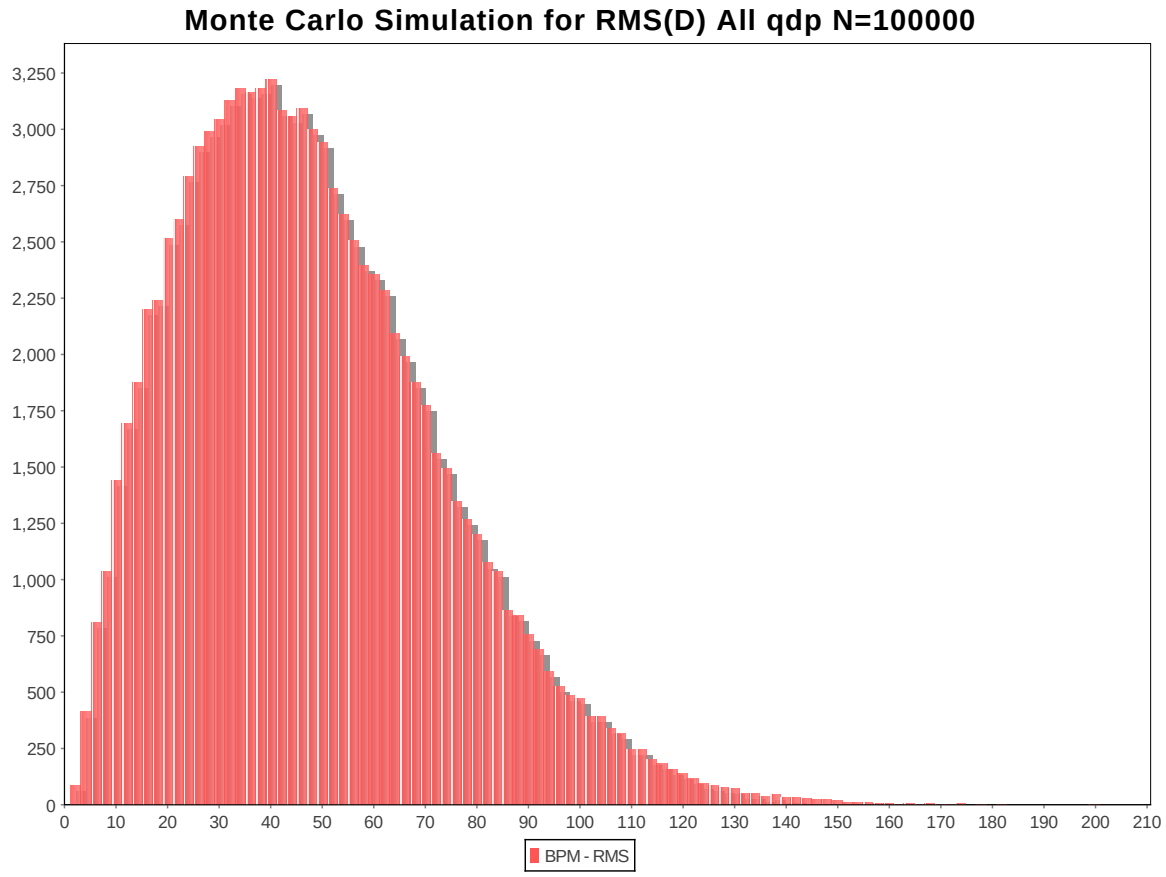

Figure 3.2.: MCS of the RMS at the BPMs for the dispersion, for $N = 100000$ and $\sigma = 0.2mm$. The value shown on the abscissa is the RMS in mm.

According to this calculation a placement of the quadrupoles with a precision of 0.2mm (resulting $RMS_D = 48mm$) would not be sufficient to achieve a gain length increase below 10% (required $RMS_D < 18mm$) due to misalignment of quadrupoles.

In the following the results of the calculation of the dispersion are compared with the PhD thesis of E.Prat [2]. The characteristic parameters were calculated for a setting in which the quadrupoles in the collimator (ECOL + TCOL: Q3ECOL Q4ECOL Q5ECOL Q2TCOL Q8TCOL Q9TCOL) were seeded with random x offsets σ only. The values for the characteristic parameters specified here have

been calculated for the undulator section of the beamline. $N = 1000$ Monte Carlo runs were done for the plots and the parameter σ (x offset of the quadrupole) was tuned from $0.1mm$ to $1.0mm$ in steps of $0.1mm$. A Monte Carlo run was performed each time interpreting σ as the standard deviation of a Gaussian distribution. The results of these series of calculations are shown in figure 3.3 for the characteristic values of the trajectory and in figure 3.4 for the characteristic values of the dispersion. The Earth's magnetic field was not considered in these calculations.

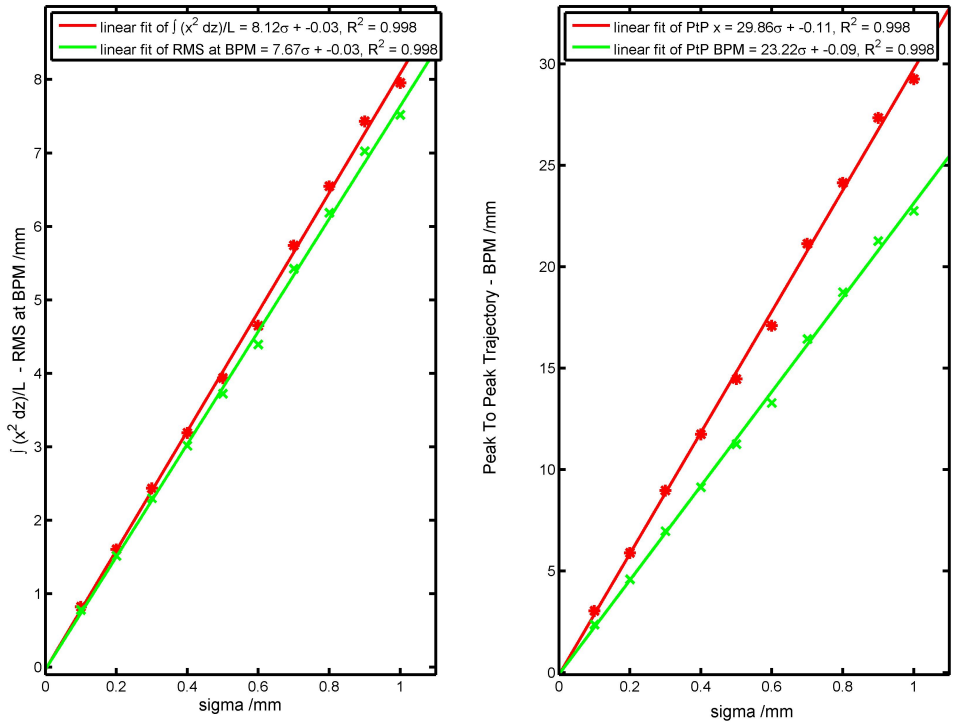

Figure 3.3.: The MCS yields values for the trajectory which scale linear with the specified x offset of the quadrupoles σ.

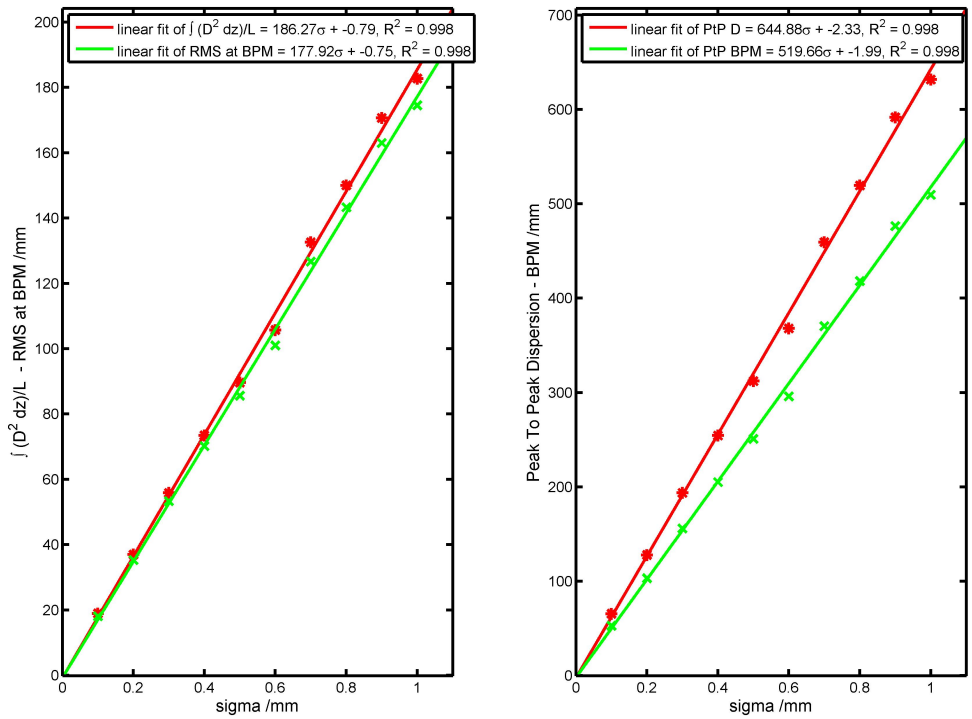

Figure 3.4.: The MCS yields values for the dispersion which scale linear with the specified x offset of the quadrupoles σ.

The values calculated by E.Prat are given in [2] page 34 Table 4.1. He calculated a required σ for the x offsets of the undulators in the collimator section of $\sigma = 76\mu m$ to generate a dispersion (RMS) in the undulator section of the beamline of $RMS_D = 10mm$.
TOP yields for a similar configuration a value of $\sigma = 60\mu m$ which is in good agreement with the existing paper.

4. Results

4.1. Comparison with experimentally measured data

The simulation has been compared with measured data by the BPM system of the FLASH beamline. This data was acquired by P. Castro et al. on 13^{th} and 21^{st} of November 2008. The simulation for $B_{earth} = -29\mu T$ which has been fitted to the measured data agrees very well with the measurement of the vertical component of the Earth's magnetic field in the FLASH tunnel of $B_{earth} = -30\mu T$. The simulated trajectory and the measured data is shown in figure 4.1 for a $504MeV$ and in figure 4.2 for a $897MeV$ beam. The second and the fifth data point plotted in the two figures were used as fitting-constraints instead of the unknown initial conditions x_0 and x_0'.

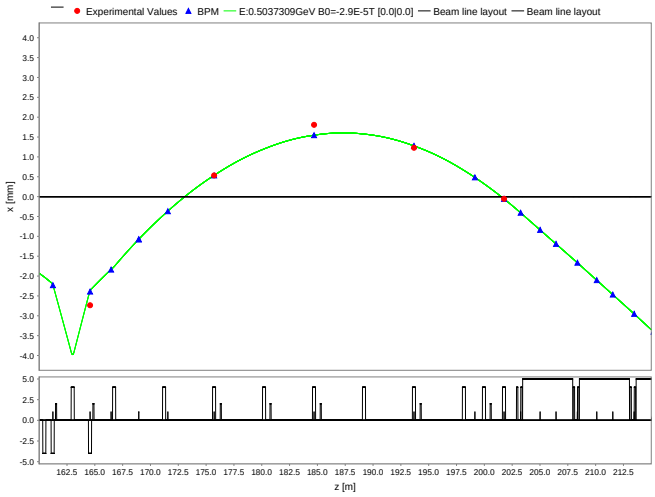

Figure 4.1.: Comparison of measured beam position and simulation for a $504MeV$ electron beam in FLASH. The red round dots represent experimentally measured data.

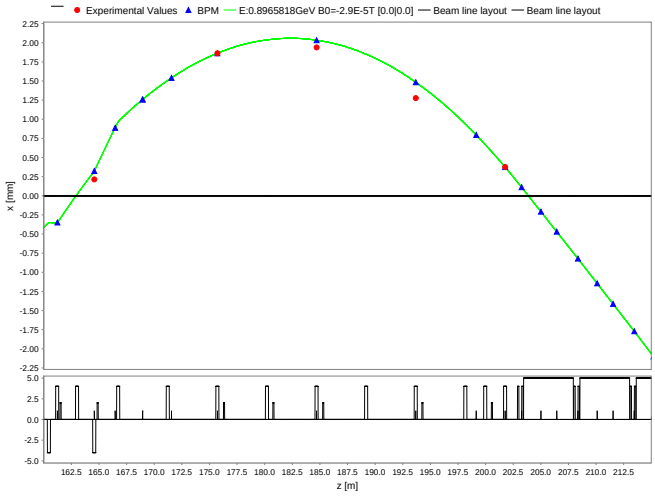

Figure 4.2.: Comparison of measured beam position and simulation for a $897MeV$ electron beam in FLASH. The red round dots represent experimentally measured data.

4.2. Initial condition at FLASH

The effect of the Earth's magnetic field on the trajectory while changing the energy is shown in figure 4.3 for quadrupole magnets turned off.

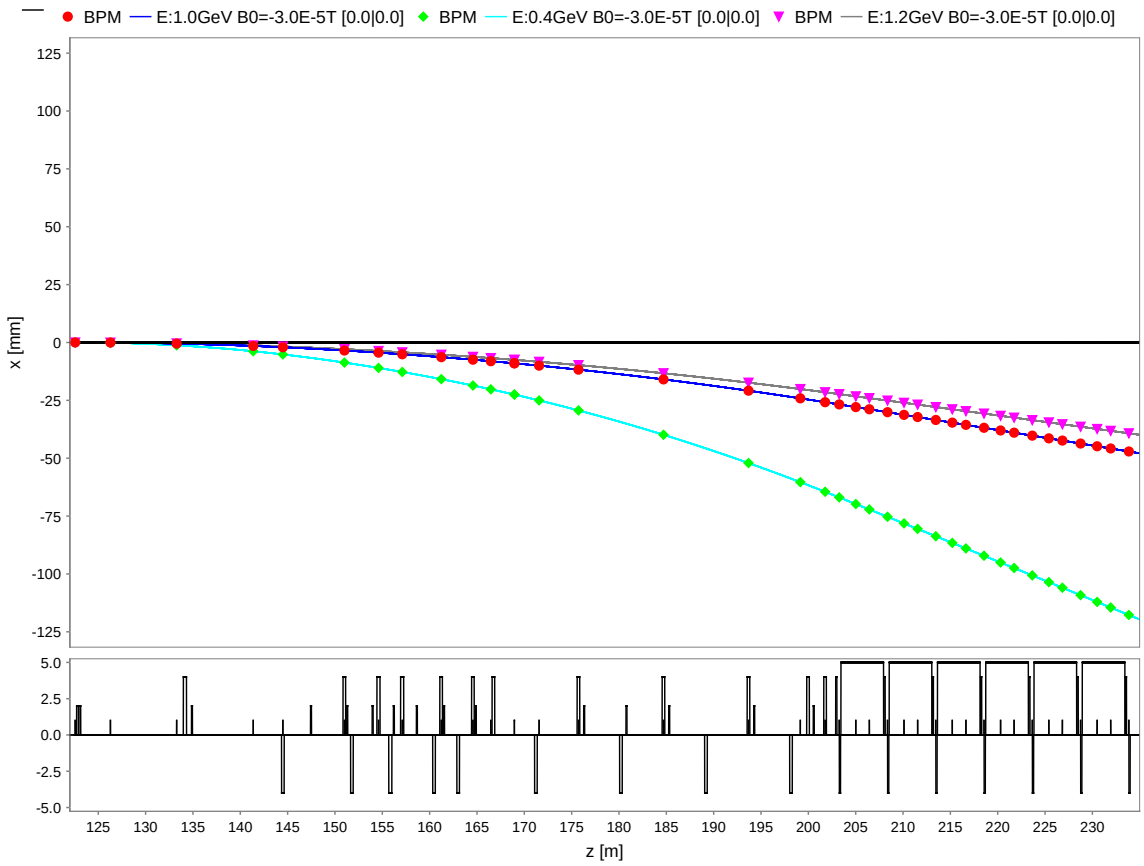

Figure 4.3.: Trajectory of FLASH's electron beam for turned off quadrupole magnets and the effects of the Earth's magnetic field while tuning the beam energy from $1.0GeV$ to $0.4GeV$ and to $1.2GeV$.

The scaling scheme for quadrupole strengths k (as described in 1.2) has been applied and the trajectory has been calculated for different energies (see figure 4.4). As one can see clearly the effect is not small and can not be neglected.

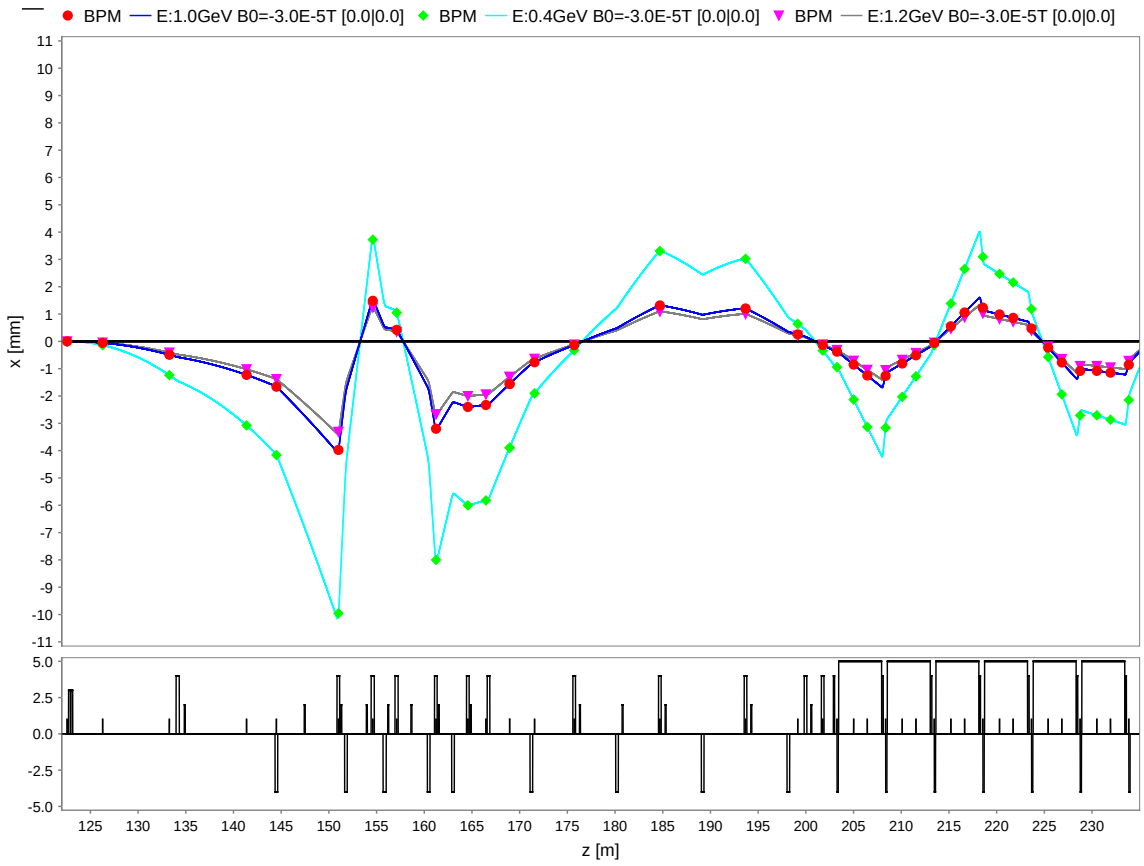

Figure 4.4.: Trajectory of FLASH's electron beam for turned on quadrupole magnets and the effects of the Earth's magnetic field while tuning the beam energy from $1.0GeV$ to $0.4GeV$ and to $1.2GeV$.

The initial condition for this simulation was $x_0 = 0$ and $x'_0 = 0$. For this setup the trajectory is a straight line at $x = 0$ when the Earth's magnetic field is not considered.

The dispersion for the initial setup is shown in figure 4.5.

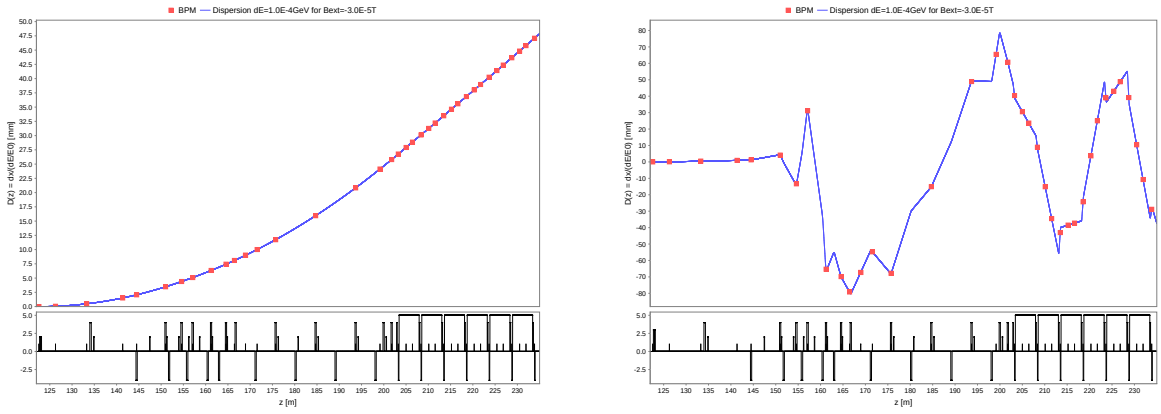

Figure 4.5.: Dispersion for initial FLASH setup. On the left: quadrupoles turned off. On the right: quadrupoles turned on.

4.3. Compensating the Earth's magnetic field

One of the main goals of this project is to find suitable corrector settings to compensate the effects of the Earth's magnetic field in the beamline. To find the optimal corrector (dipole) magnetic fields (i.e. the corrector currents) different strategies are applied.

In the following the general idea for compensating the Earth's magnetic field is given. Several methods based on this idea are developed. At the end of the chapter the results of the discussed methods are presented.

A) General idea for an optimization using constraints

The most straight forward algorithm to set N corrector currents for compensating an external magnetic field would be just to fix the x coordinate at N given constraint points to a certain value. This would yield N equations for N variables (the corrector currents). This approach will not yield the optimal trajectory but certainly a compensation for the external field will be achieved.
The choice of the constraint points (in z position) was set to the location of the correctors and the constraining x value to zero. The constraint of corrector m will be that the trajectory produced by the current of this corrector has to fulfill $x = 0$ at the z position of corrector $m + 1$. For the last corrector (N) the end of the beamline will be used as the position for the constraint.

B) Sequential Optimization (SO)

To implement the idea specified above one can calculate the trajectory just from the beginning to corrector m for $I_{m,0} = 0A$ and for $I_{m,0} = 1A$. Because the x position depends linearly on the current I it is possible to calculate the current $I_{m,opt}$ for this corrector to meet the constraining condition. This can be done using the equation for a linear function

$$x = k \cdot I + d \tag{4.1}$$

$$k = \frac{\Delta x}{\Delta I} \tag{4.2}$$

$$d = x_0 \tag{4.3}$$

where Δx is the change in horizontal position and ΔI is the change in current. As $I_{m,1} = 1A$ and $I_{m,0} = 0A$ (where the sub indices 1 and 0 always label the two calculated trajectories according to the applied current I) one gets for k

$$k = x_1 - x_0 \tag{4.4}$$

Putting everything together the optimal current $I_{m,opt}$ can be calculated by

$$I_{m,opt} = -\frac{x_{m+1,0}}{x_{m+1,1} - x_{m+1,0}} \tag{4.5}$$

This approach has certain difficulties with the special condition that some correctors can be linked to each other by having the same power supply. This means they have to be optimized at once having the same current.
To cope with this additional restrictions and have a more general tool for different calculations the concept of the trajectory response table is introduced in the next section.

C) Trajectory Response Table (TRT)

In many problems we deal with, the effects of a certain beamline element (for example a corrector) on a initially given trajectory are to be examined.
In the following a TRT only for correctors is discussed. The TRT for correctors is built in the following way: at first the initial trajectory is calculated for the whole beamline with all effects one wants to consider. The currents for the correctors have to be all zero. Then the whole trajectory is calculated for each corrector set to $1A$ while all others are at $0A$. All disturbing effects like external fields have to be turned off in this calculation because they are already included in the initial trajectory.

In this case one can exploit the linearity of the magnetic fields to calculate the effects of the correctors on the initial trajectory

$$\vec{x}_{new} = \vec{x}_{initial} + \sum_{m}^{N} \vec{x}_m \cdot I_m \tag{4.6}$$

$$\vec{x'}_{new} = \vec{x'}_{initial} + \sum_{m}^{N} \vec{x'}_m \cdot I_m \tag{4.7}$$

where m is the index of the corrector running from 1 to the number of correctors available N. Using this one can see that it is possible to investigate the effects of any current configuration for the correctors on any given initial trajectory by superposition of the TRT vectors.
Having the TRT at hand for a given beamline and settings it is easy to implement the optimization for the corrector currents for the constraint setup mentioned above and constraint values x set to zero

$$I_{m,opt} = -\frac{x_{m+1,0}}{x_{m+1,1}} \tag{4.8}$$

It is worth to mention here that optimization of corrector m is not independent of the optimizations of correctors ($m-1$, $m-2$, ...). In fact the starting coordinates for the trajectory at m are determined by the preceding steps. This is taken into account naturally by a sequential approach. Using the TRT you have to update your initial trajectory after each optimized corrector using equation 4.7 before calculating the following ($m+1$, $m+2$, ...) correctors. Therefore it is not possible to optimize corrector $m+i$ before the effects of corrector m were taken into account. This is clear for a sequential approach but using this superposition one might be tempted to use the TRT entries in any order, which is not possible.

Using this method it is also easy to account for two correctors having the same power supply (if they are right next to each other) by just calculating only one TRT entry for these two and treating them virtually as one corrector.

D) Second Iteration Approach (SI)

Using the results of the TRT approach the next step is to look for improvements to this basic scheme. The parameters which are easy to tune in this model are

- the z position of the constraints
- the x value at the constraint positions
- the constraint variable (using x' instead of x)

The most promising idea was to modify the value of the x constraints. The approach given here is based on a somewhat dynamical choice of the x constraints based on a first iteration.

In a first iteration the TRT optimization process is done as explained above using the standard condition $x|_{Constr.} = 0$. The calculated set of currents $\vec{I}$ will be neglected from now on and just the resulting trajectory is used to determine the maxima $\vec{x}_{max}$ of the trajectory between each two constraints.
This set of N maxima $\vec{x}_{max}$ will be used in a second iteration of the same process but this time the constraint for x will not be zero any longer but the maximum $\vec{x}_{max,m}$ scaled by some factor.

$$\vec{c} = \frac{\vec{x}_{max}}{f} \tag{4.9}$$

where $\vec{c}$ is the vector of new x constraints and f is an yet arbitrary scaling parameter. The idea is that f takes on values between 1 and ∞ to shift the constraint from the initial zero to a maximum value for $x|_{Constr.}$ which is $\vec{x}_{max,m}$.

An analytical attempt has been made to find the optimal value for the scaling factor f (see appendix C). The analytical value obtained is $f_{opt,A} = 1$. Simulations show that the value in our case is $f_{opt,N} = 1.36$.

E) Second Iteration Approach with special conditions (SISC)

The constraint of the last corrector has to be different because the undulator section following this element needs special treatment. In the undulator section it is vital that the angle of the trajectory is not changed to achieve a good SASE process. So the angle x' is used as the variable for constraining the current of the last corrector and the z position for the constraint is the z position right after the end of the corrector.

The SI approach is used for the whole beamline except for the last corrector where the new condition

$$x'|_c = x'_{miss} + x'_{offset} = x'_{initial} + x'_N \cdot I_N \tag{4.10}$$

$$I_N = -\frac{x'_{initial} - x'_{offset}}{x'_N} \tag{4.11}$$

is applied without any second iteration.
In this equation I_N is the current of the last corrector, $x'_{initial}$ and x'_N are the values of the angle of the initial trajectory and the response trajectory of the last corrector at the z position right after the end of the last corrector and x'_{offset} is an artificial angle to compensate the remaining influence of the Earth's magnetic field in the undulator section.

The parameter x'_N is unpredictable for arbitrary undulator sections. A value was found for the given configuration which is $x'_N = 15\mu rad$. Since we do not want to be limited to a specific beamline layout a different approach for the last corrector has to be used (see below: G) Final approach using constraints).

F) Using existing numerical minimization algorithms

In addition to the method described above several minimization algorithms have been tested (Minuit, Matlab built-in, ...). For a detailed description of numerical minimization procedures (Fibonacci grid search, gradient methods, ...) see [6].

G) Final approach using constraints

The final approach used consists of the two iteration method (SI) (described in D) for all correctors except for the last one. For the last corrector the fitting tool JMinuit is used to minimize the quadratic integral of the trajectory produced by the last corrector. In the following when we refer to method SI this setup was used.

The results for the characteristic parameters for several optimization schemes are given in table 4.1 and table 4.2. The characteristic parameters for the trajectory (table 4.1) are calculated for the collimator and diagnostics section of the beamline. The characteristic parameters for the dispersion (table 4.2) are calculated for the undulator section of the beamline. In the tables the initial condition is shown as well as the SI approach for different values of f. The last four lines are methods using numerical minimization algorithms JMINUIT and FMINUNC. The three options specified at FMINUNC represent the quantity which was minimized: intT - the quadratic integral of the trajectory, PtPT - the peak to peak value of the trajectory, cmb - a combination of both. It turned out that the best results are achieved by using only the quadratic integral of the trajectory as the quantity to minimize.

Table 4.1.: Series of simulations to find the optimal method for compensating the Earth's magnetic field for characteristic parameters related to the trajectory x. The characteristic parameters were calculated for the collimator and diagnostics section of the beamline.
Method ... Method used for calculating the corrector currents.
$\sqrt{\frac{\int x^2 dz}{L}}$ ... Quadratic integral of the trajectory normalized by the trajectory length.
RMS of x at BPM ... Root mean square of x positions at BPM positions.
Peak to Peak x ... Peak to Peak value of the trajectory.
Peak to Peak x at BPM ... Peak to Peak value of the trajectory at the BPMs.

Method	$\sqrt{\frac{\int x^2 dz}{L}}$ mm	RMS of x at BPM mm	Peak to Peak x mm	Peak to Peak x at BPM mm
initial	1.394	1.646	5.532	5.456
f = inf	0.072	0.069	0.160	0.154
f = 6	0.063	0.061	0.173	0.133
f = 5	0.061	0.059	0.175	0.129
f = 4	0.058	0.057	0.180	0.126
f = 3	0.055	0.054	0.186	0.127
f = 2	0.049	0.048	0.200	0.138
f = 1.69	0.047	0.046	0.208	0.144
f = 1.5	0.046	0.044	0.215	0.149
f = 1.36	0.045	0.043	0.221	0.154
f = 1.25	0.046	0.043	0.227	0.158
f = 1	0.050	0.044	0.246	0.171
f = 0.75	0.066	0.054	0.280	0.193
f = 0.5	0.110	0.087	0.356	0.251
JMINUIT	0.057	0.063	0.257	0.209
intT FMINUNC	0.040	0.037	0.235	0.148
PtPT FMINUNC	0.076	0.076	0.170	0.159
cmb FMINUNC	0.062	0.059	0.170	0.153

Table 4.2.: Series of simulations to find the optimal method for compensating the Earth's magnetic field for characteristic parameters related to the dispersion D. The characteristic parameters were calculated for undulator section of the beamline.
Method ... Method used for calculating the corrector currents.
$\sqrt{\frac{\int D^2 dz}{L}}$ ... Quadratic integral of the dispersion normalized by the trajectory length.
RMS of D at BPM ... Root mean square of dispersion at BPM positions.
Peak to Peak D ... Peak to Peak value of the dispersion.
Peak to Peak D at BPM ... Peak to Peak value of the dispersion at the BPMs.

Method	$\sqrt{\frac{\int D^2 dz}{L}}$ mm	RMS of D at BPM mm	Peak to Peak D mm	Peak to Peak D at BPM mm
initial	32.739	31.104	110.575	91.799
f = inf	0.079	0.073	0.315	0.266
f = 6	0.065	0.061	0.260	0.219
f = 5	0.063	0.059	0.250	0.210
f = 4	0.060	0.056	0.235	0.197
f = 3	0.055	0.052	0.209	0.175
f = 2	0.049	0.046	0.195	0.157
f = 1.69	0.047	0.045	0.196	0.157
f = 1.5	0.047	0.046	0.191	0.154
f = 1.36	0.049	0.047	0.196	0.156
f = 1.25	0.050	0.049	0.195	0.155
f = 1	0.060	0.059	0.213	0.162
f = 0.75	0.085	0.083	0.315	0.242
f = 0.5	0.145	0.140	0.522	0.415
JMINUIT	0.434	0.415	1.384	1.155
intT FMINUNC	0.172	0.163	0.553	0.454
PtPT FMINUNC	0.594	0.560	2.245	1.764
cmb FMINUNC	0.166	0.160	0.616	0.470

As one can see in table 4.1 and 4.2 independent of the optimization method applied the resulting characteristic parameters improve by two orders of magnitude. Due to the fact that the quantity which was minimized was always related to the trajectory, the results of the numerical optimization methods are inferior to the SI approach for the dispersion values.

The resulting curves for the quadratic integral of the trajectory (on the top: collimator and diagnostics section) and of the dispersion (in the middle: collimator and diagnostics section, on the bottom: undulator section) are shown in figure 4.6. The two datasets shown in the right part of the figure show the results of JMINUIT and FMINUNC for the optimization. The results of JMINUIT may be not as good as expected due to problems we had with getting the method to converge. Default parameters and zero initial values were the only options converging at all. FMINUNC was the optimization routine which yielded the best results out of several methods (FMINCON, FMINUNC, FMINSEARCH, SIMPLEX, CSMINWEL NUM) which were tested in Matlab.

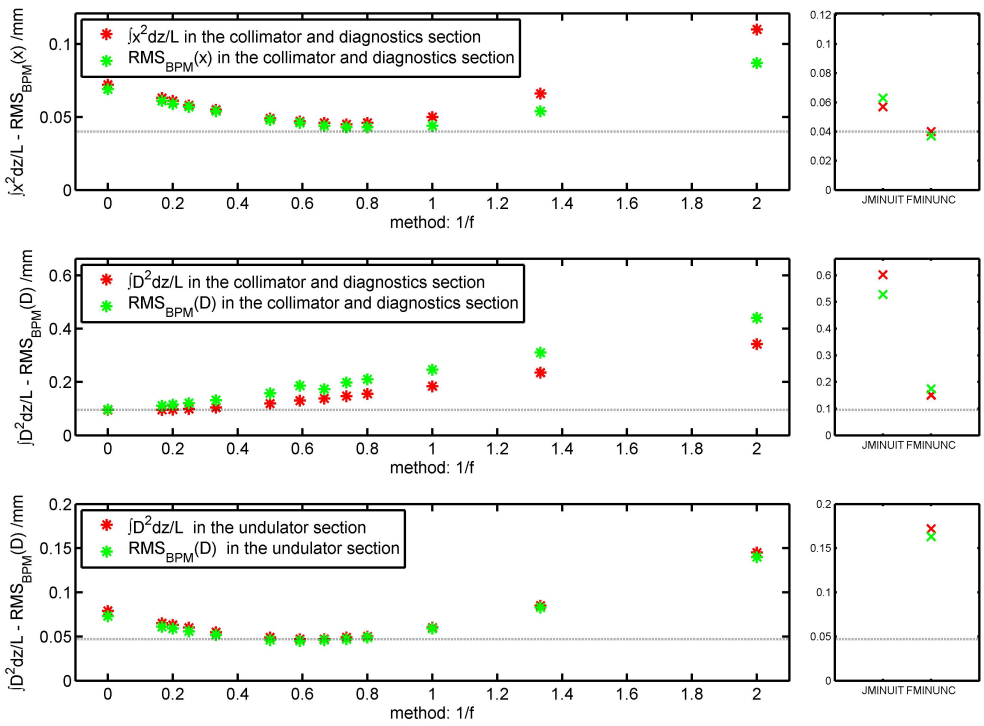

Figure 4.6.: The characteristic parameters of the trajectory and of the dispersion for different optimization approaches. In the top part: characteristic parameters for the trajectory calculated for the collimator and diagnostics section. The minimum of the quadratic integral of the trajectory is reached with method FMINUNC. The best value for the constraint approach is achieved with method $f = 1.36$. In the middle part: characteristic parameters of the dispersion calculated for the collimator and diagnostics section. The minimum of the quadratic integral of the dispersion is achieved with method $f = \infty$. In the bottom part: characteristic parameters of the dispersion calculated for the undulator section. The minimum of the quadratic integral of the dispersion is achieved with method $f = 1.69$. Note that the values for JMINUIT are too high so they are not shown in this part.

Considering all the results three different strategies are suggested as being optimal (see figure 4.6). Depending on which characteristic parameter you consider more important (compared are characteristic parameters for the trajectory in the collimator and diagnostics section and characteristic parameters for the dispersion in the undulator section)

1. $\sqrt{\frac{\int x^2 dz}{L}} > \sqrt{\frac{\int D^2 dz}{L}}$
   use the SI approach: $f = 1.36$ or FMINUNC
   The resulting trajectory is given in figure 4.7 for $f = 1.36$ and in figure 4.8 for FMINUNC.

2. $\sqrt{\frac{\int x^2 dz}{L}} < \sqrt{\frac{\int D^2 dz}{L}}$
   use the SI approach: $f = 1.69$
   The resulting trajectory is given in figure 4.9.

The result for the characteristic parameters for these three methods are listed (amongst others) in table 4.1 and table 4.2. The x-x' phase space of the initial situation and the compensation (method $f = \infty$) is discussed in appendix D. The results for the optimal currents for each of the three selected methods are shown in table 4.3.

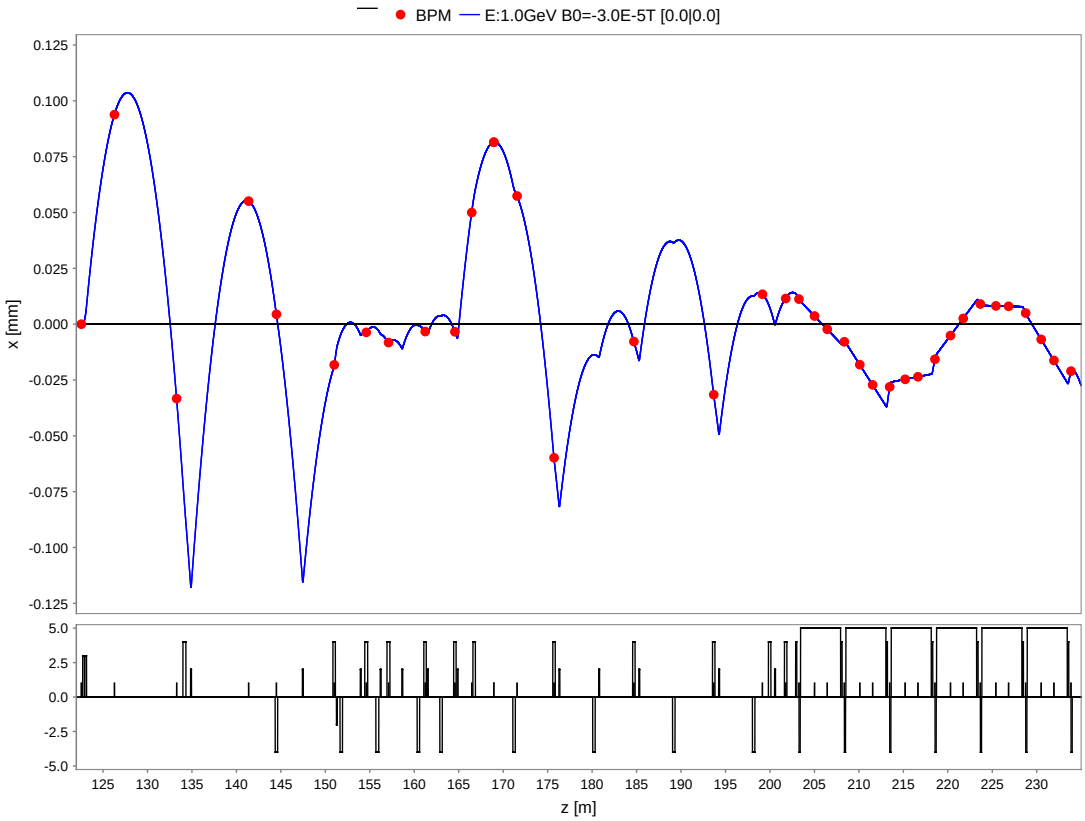

Figure 4.7.: Trajectory for compensation method $f = 1.36$.

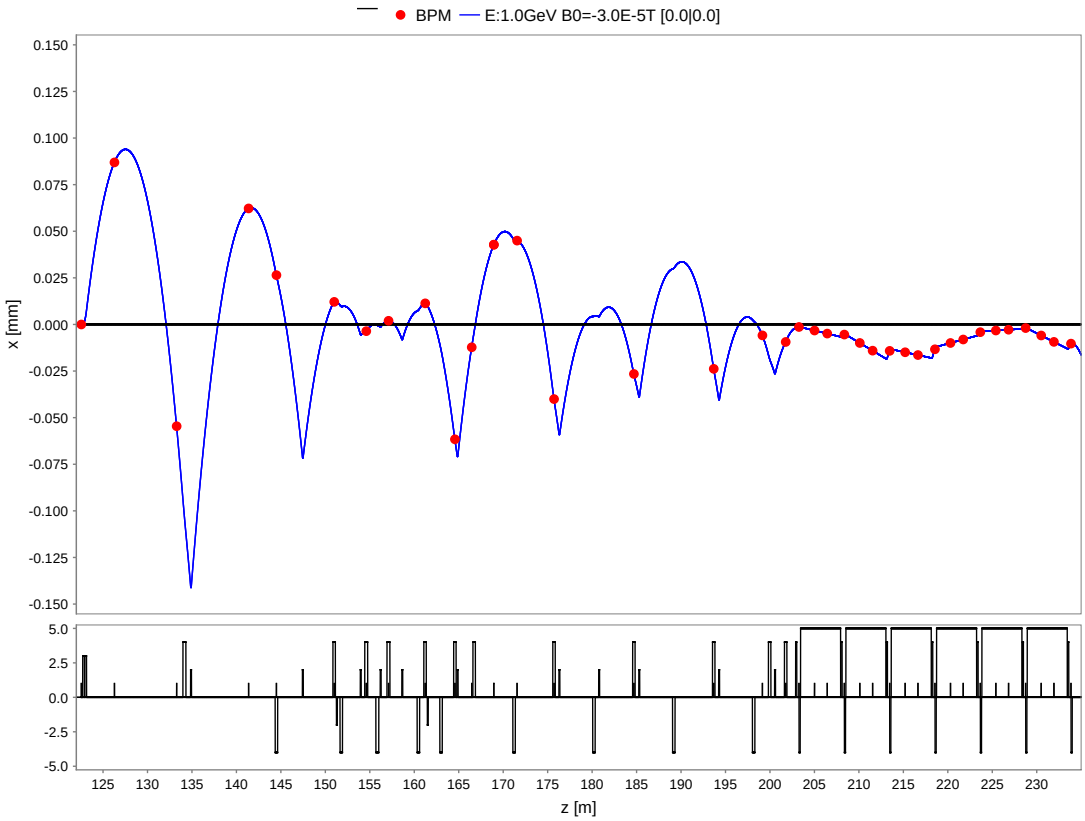

Figure 4.8.: Trajectory for compensation method intT FMINUNC.

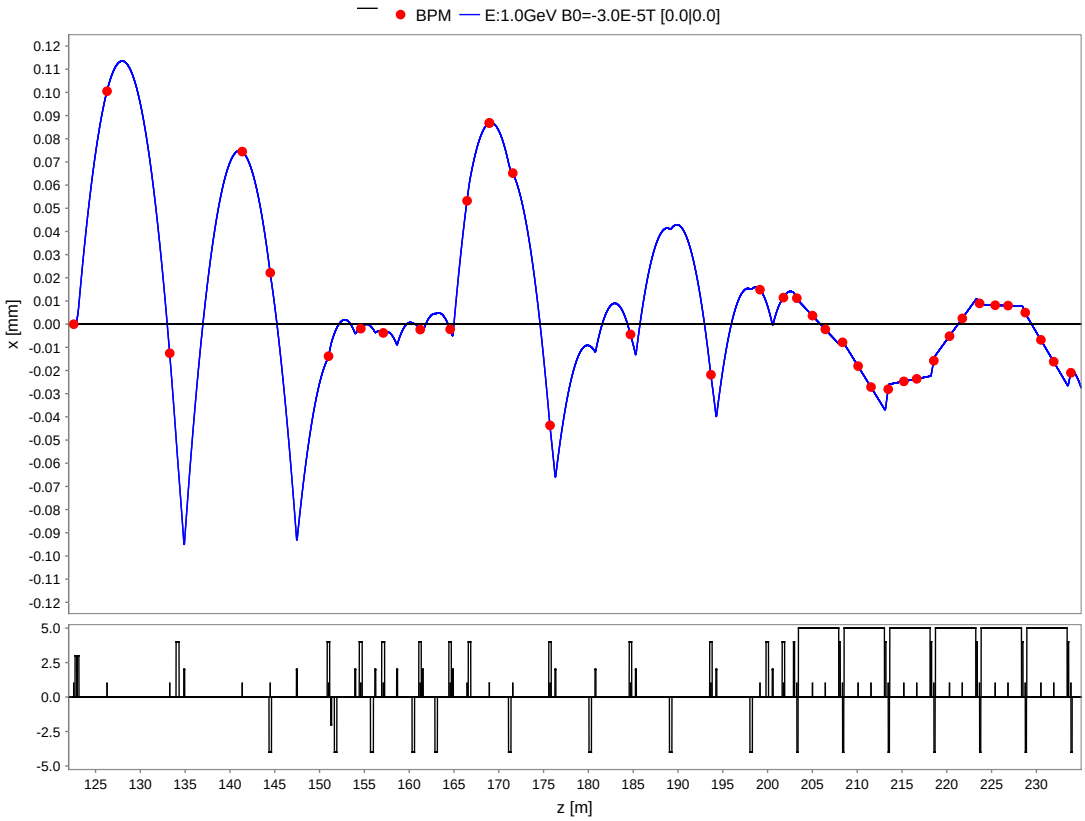

Figure 4.9.: Trajectory for compensation method $f = 1.69$.

Table 4.3.: Calculated corrector currents to compensate the Earth's magnetic field for the three final methods.
Corrector ... Name of the corrector.
$f = 1.36$ ... Calculated currents in mA for method $f = 1.36$.
FMINUNC ... Calculated currents in mA for method FMINUNC.
$f = 1.69$ ... Calculated currents in mA for method $f = 1.69$.

Corrector	$f = 1.36$ mA	FMINUNC mA	$f = 1.69$ mA
H9ACC6	530.9	506.2	555.0
H10ACC6	530.9	506.2	555.0
H10ACC7	590.9	618.5	585.7
H4TCOL	33.7	29.9	31.4
H9TCOL	-4.4	-1.0	-1.8
H2ECOL	57.7	90.0	64.6
H4ECOL	25.6	45.7	42.6
H6ECOL	89.3	123.1	93.7
H3MATCH	5.5	-0.8	5.8
H6MATCH	18.7	27.1	19.1
H5SUND2	25.7	23.8	24.9
H4SUND3	8.1	4.1	9.0
H3SEED	16.6	20.3	16.8
H12SEED	22.8	20.4	22.3
H19SEED	10.8	12.2	11.2

5. Conclusion

A simulation program (TOP) has been developed for calculating trajectories, optimizing corrector currents, doing MCS on quadrupole offsets, ... (see [4]).

The results of this newly developed simulation have been compared with existing programs and measurements and the agreement was found to be very good in all cases (see chapter 3).

The effects of the Earth's magnetic field on the electron trajectory in FLASH have been studied. A scheme has been developed to compensate them as good as possible (see section 4.3).

The new scheme for altering the beam energy at FLASH suggested is:
The quadrupole currents should be transformed according to

$$\vec{I}_{q,new} = \frac{E_{new}}{E_{initial}} \vec{I}_{q,initial} \tag{5.1}$$

to keep the quadrupole strength k constant. The corrector currents should be changed according to

$$\vec{I}_{c,initial} = \vec{I}_c^{OTHER} + \vec{I}_c^{EARTH} \tag{5.2}$$

$$\vec{I}_{c,new} = \frac{E_{new}}{E_{initial}} (\vec{I}_{c,initial} - \vec{I}_c^{EARTH}) + \vec{I}_c^{EARTH} \tag{5.3}$$

to keep the bending radius ρ constant and correctly account for the constant magnetic field of the Earth.
The calculated values for the compensating currents $\vec{I}_c^{EARTH}$ are given in table 4.3.

Three different optimization methods have been identified to yield good results for the compensation (see section 4.3).

The optimal compensation of the Earth's magnetic field improves the values for the trajectory RMS from $1.394mm$ to $0.045mm$ (decrease by a factor of 15) and those of the dispersion RMS in the undulator section $\sqrt{\frac{\int D(z)^2 dz}{L}}$ from $32.739mm$ to $0.047mm$ (decrease by a factor of 700). The resulting dispersion is well below the value of tolerance ($18mm$) for a 10% increase in gain length. These improvements are given with respect to the considered inital trajectory where all correctors were turned off.

The improvement, using the new scheme of changing the energy instead of the old procedure, is shown in the following.
The quantity Δx is plotted in figure 5.1 as a function of z. The reference energy has been $1GeV$. The energy has been tuned to $0.4GeV$ and to $1.2GeV$ to study the change of the orbit. The result of scaling with equations 1.1 and 1.2 is shown in figure 5.1 (left). The result of scaling with equations 5.1 and 5.3 using the compensating currents of table 4.3 is shown in figure 5.1 (right). Note the different vertical scale. The RMS value of Δx for the curves shown for $0.4GeV$ is $1.9mm$ for the left plot and $0.1mm$ for the right plot. The RMS value of Δx for the curves shown for $1.2GeV$ is $0.21mm$ for the left plot and $0.01mm$ for the right plot.

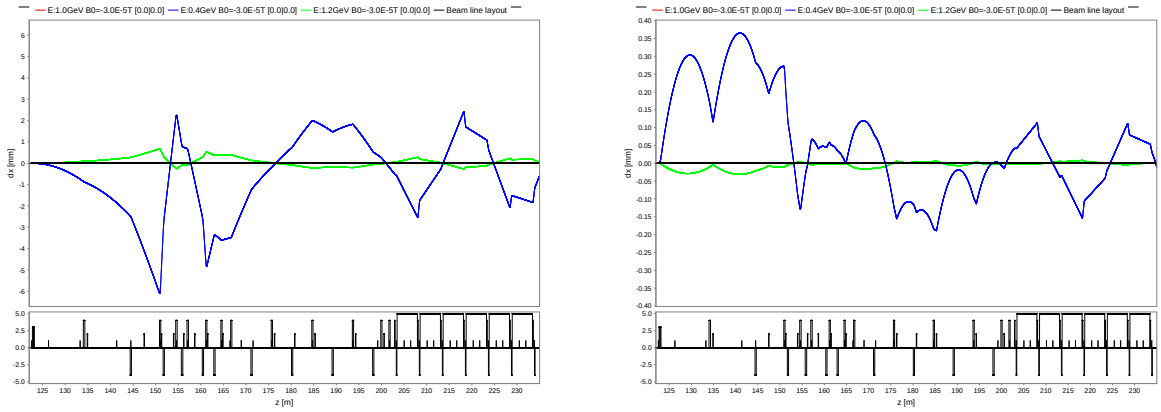

Figure 5.1.: Effect of the applied compensation for the Earth's magnetic field. Shown is the difference in the horizontal direction x for a trajectory for $E = 1.2GeV$ and for a trajectory for $0.4GeV$ with respect to a reference setup for $E = 1.0GeV$. On the left: The initial situation. On the right: The situation with applied compensation (method $f = \infty$). Note the different vertical scale (a factor of 15).

Acknowledgement

I would like to thank the organizers of the DESY summer student program for a great opportunity and for a really good summer I was allowed to spend in Hamburg. Especially I want to say thank you to Prof. Joachim Meyer for great lectures and for being always available for information of all kind. Also for giving me the possibility to work exactly on the topic I am curious about, which is FLASH. I thank my supervisor Dr. Pedro Castro very much. He chose a very interesting and appropriate project for this summer. On working on his tasks I was able to learn a lot. I am very grateful for his advice on how to solve all kinds of problems and on how to improve my report. I wish to thank him for help and encouragement, the huge amount of time he spent on explaining ideas to me and the insights he provided into the very interesting subject of accelerator physics. Finally I want to thank my colleague Agnieszka Priebe for the lots of fun we had and the many inspiring chats and valuable discussions about our projects.

Bibliography

[1] DESY: FLASH homepage. 2009. http://flash.desy.de/accelerator/ : DESY, 2009

[2] Prat, E: Spurious Dispersion Effects at FLASH. 1. Universität Hamburg, 2009

[3] Wiedemann, H: Particle Accelerator Physics. 3. Springer, 2007

[4] Nuss, M: TOP Documentation. 1. http://tesla.desy.de/~pcastro/TOP/documentation.pdf : DESY, 2009

[5] Schmidt, F: MAD-X User's Guide. 2.12. CERN, 2003

[6] James, F: MINUIT Tutorial Function Minimization. 2004. http://seal.web.cern.ch/seal/documents/minuit/mntutorial.pdf : CERN, 2004

[7] Dreizler, R: Theoretische Physik 2 - Elektrodynamik und spezielle Relativitaetstheorie. Springer, 2005

[8] Chao, A: Handbook of Accelerator Physics and Engineering. 2. World Scientific, 1998

[9] Hinterberger, F: Physik der Teilchenbeschleuniger und Ionenoptik. 1. Springer, 1997

[10] Brefeld, W: Formulas for accelerator physics. 2001. http://hasylab.desy.de/facilities/sr_and_fel_basics/sr_basics/index_eng.html : DESY, 2001

List of Figures

List of Tables

A. Nomenclature

- BPM ... Beam Position Monitor
- FEL ... Free Electron Laser
- FLASH ... Free Electron LASer in Hamburg
- LASER ... Light Amplification by Stimulated Emission of Radiation
- LINAC ... LINear ACCelerator
- MCS ... Monte Carlo Simulation
- RF ... Radio Frequency
- SASE ... Self Amplified Stimulated Emission
- TMF ... Transport Matrix Formalism
- TOP ... Trajectory Optimization Program (The name of the simulation program which has been developed.)
- TRT ... Trajectory Response Table
- VUV ... Vacuum Ultra Violet

B. Characteristic Parameters

The parameters introduced here will be referred to as characteristic parameters throughout this paper.
To get an impression for the quality of the calculated trajectory the following parameters are calculated for the part of the beamline of interest ($x(z)$ is the horizontal beam position and $D(z) = \frac{dx(z)}{\frac{dE}{E_0}}$ is the dispersion):

1. The quadratic integral of the trajectory divided by the length. $\sqrt{\frac{\int x(z)^2 dz}{L}}$
2. The RMS of the trajectory at the position of the BPMs $\sqrt{\frac{\sum x^2}{N}}$
3. The peak to peak value of the trajectory. $|max(x) - min(x)|$
4. The peak to peak value of the trajectory at the BPMs. $|max_{BPM}(x) - min_{BPM}(x)|$
5. The quadratic integral of the dispersion divided by the length. $\sqrt{\frac{\int D(z)^2 dz}{L}}$
6. The RMS of the dispersion at the position of the BPMs $\sqrt{\frac{\sum D^2}{N}}$
7. The peak to peak value of the dispersion. $|max(D) - min(D)|$
8. The peak to peak value of the dispersion at the BPMs. $|max_{BPM}(D) - min_{BPM}(D)|$

All of these have the dimension length and will be given in mm.
The RMS values are introduced because these values correspond to the values seen on displays in the control room and so they are convenient for comparison. By random sampling the values of the quadratic integrals and the RMS values agree pretty well.

C. Analytical calculation of f_{opt}

We want to determine the optimal scaling factor f for the second iteration approach (SI) described in chapter 4.3. One can not easily see the optimal value for f.
In order to calculate an analytical f_{opt} we have to make some assumptions and simplifications. We consider just one corrector at position $z = 0$ and its constraint a distance L away. There are no elements (quadrupoles, undulators, ...) in between the corrector and the constraint position. So the whole space is just a drift space with external magnetic field.
The trajectory for such conditions can be modeled as a second order polynomial

$$x = Bz^2 + Cz + X_0 \tag{C.1}$$

The constant $B < 0$ is proportional to the strength of the Earth's magnetic field, the constant C is proportional to the corrector current and the constant X_0 is just the x starting location at the position of the corrector which we set to zero.
The first task now is to calculate the value of the maximum of the trajectory for the constraint that x at $z = L$ is zero (like in the initial TRT approach). First expressing the constraint

$$\begin{aligned} x(L) &= 0 = B \cdot L^2 + C^0 \cdot L && \text{(C.2)} \\ &\Rightarrow C^0 = -B \cdot L && \text{(C.3)} \end{aligned}$$

To find the maximum of the function C.1 we plug in relation C.3, differentiate and set the result equal to zero, which yields

$$\begin{aligned} x &= Bz^2 + C^0 z && \text{(C.4)} \\ \frac{\partial}{\partial z} x(z) &= 2Bz - BL \stackrel{!}{=} 0 && \text{(C.5)} \\ &\Rightarrow z^0_{max} = \frac{L}{2} && \text{(C.6)} \\ &\Rightarrow x^0_{max} = -\frac{BL^2}{4} = \frac{C^0 L}{4} && \text{(C.7)} \end{aligned}$$

Now we know the maximal amplitude which the TRT calculation yields for this element. The next step is to apply the second iteration and calculate the quadratic integral of the trajectory (which is the quantity which should be minimal) for this approach. We again start with expressing the constraint using relation C.7

$$\begin{aligned} x(L) &= -\frac{x^0_{max}}{f} = B \cdot L^2 + C^f \cdot L && \text{(C.8)} \\ &\Rightarrow C^f = BL \cdot [\frac{1}{4f} - 1] && \text{(C.9)} \end{aligned}$$

where f is the scaling parameter we want to optimize in the end.
The quadratic integral for the trajectory using the in equation C.9 specified constant C^f is

$$\begin{aligned} I^f_{sq} &= \int_0^L x(z)dz && \text{(C.10)} \\ I^f_{sq} &= \int_0^L [Bz^2 + C^f z]^2 dz && \text{(C.11)} \\ I^f_{sq} &= \int_0^L [Bz^2 + BL \cdot [\frac{1}{4f} - 1]z]^2 dz && \text{(C.12)} \\ I^f_{sq} &= \frac{B^2 L^5}{48} \cdot [\frac{1-2f}{f^2}] + \frac{B^2 L^5}{30} && \text{(C.13)} \end{aligned}$$

The only thing left now is to minimize the integral

$$\frac{\partial}{\partial f} I_{sq}^{f} = \frac{B^2 L^5}{24} \cdot \left(\frac{f-1}{f^3}\right) \stackrel{!}{=} 0 \tag{C.14}$$

$$\Rightarrow \quad f_{opt,1} = 1 \tag{C.15}$$

$$\Rightarrow \quad f_{opt,2} = 0 \tag{C.16}$$

The solution $f_{opt} = 0$ is not a real extremum because the function diverges at that point.
The solution $f_{opt} = 1$ is a minimum due to

$$\frac{\partial^2}{\partial f^2} I_{sq}^{f} = \frac{B^2 L^5}{24} \cdot \left(\frac{3-2f}{f^4}\right) \tag{C.17}$$

$$\frac{\partial^2}{\partial f^2} I_{sq}^{f}|_{f=1} = \frac{B^2 L^5}{24} > 0 \tag{C.18}$$

The process and result of this analytic approach is visualized in figure C.1 (in arbitrary units with all constants set to 1). As indicated in the figure on the left the value for the integral for $f \to \infty$ converges to the value of the initial one iteration approach ($x_{constraint} = -\frac{x^0_{max}}{f}$, $f \to \infty$, $x_{constraint} \to 0$). The plot also shows that the integral diverges for $f \to 0$ and that the optimal integral is reached for $f = 1$.

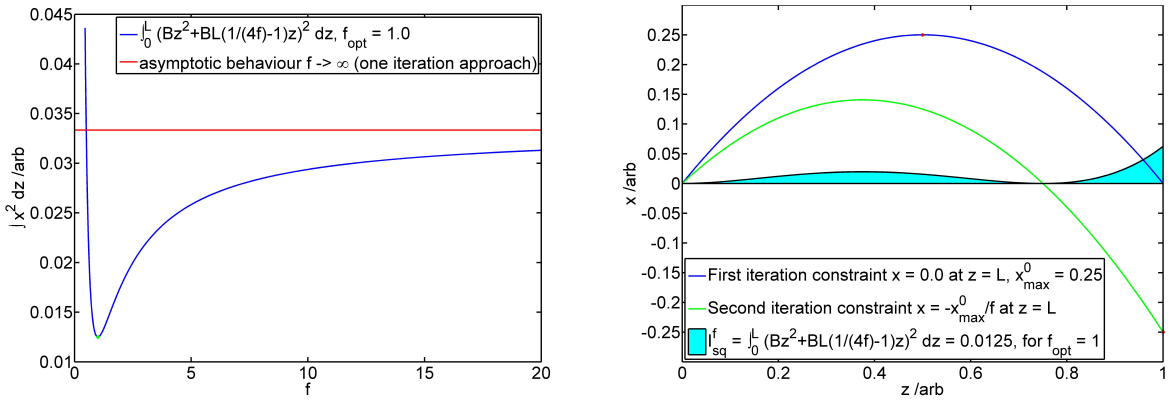

Figure C.1.: Analytically calculated behaviour for the scaling parameter f in a simplified model. On the left: Value of the quadratic integral of the trajectory as a function of the scaling parameter f. The curve of the numerical simulation is given in figure 4.6. On the right: Visualization of the considered analytical approach.

However this simplified model has serious flaws. Firstly to neglect the other beamline elements in the considered section is a crude simplification and secondly and most importantly the starting point for the next corrector will not be $X_0 = 0$ but the new constraint value.
The value for f_{opt} determined by numerical simulation for our special layout and setting is $f_{opt} = 1.36$ (see section 4.3).

D. x-x' Phase Space

As a visualization for the compensation process of the Earth's magnetic field the x - x' phase space of the trajectory with correctors turned off is shown in figure D.1. The x - x' phase space of the trajectory with applied compensation of the Earth's magnetic field (method $f = \infty$) is shown in figure D.2. Note the different scale on both axes of the two figures.
In the first picture the correctors are turned off ((green) corrector lines are perfectly horizontal (i.e. the correctors do not change the angle). In the second picture the (green) corrector lines are very steep and all starting at $x = 0$. By this one can tell that all constraints in the optimization process were set to $x = 0$ and that the correctors are turned on now. The height of the (green) corrector line is proportional to the applied corrector current. It is also visible that the Earth's magnetic field was not considered within the undulators (purple) because these are always horizontal lines.

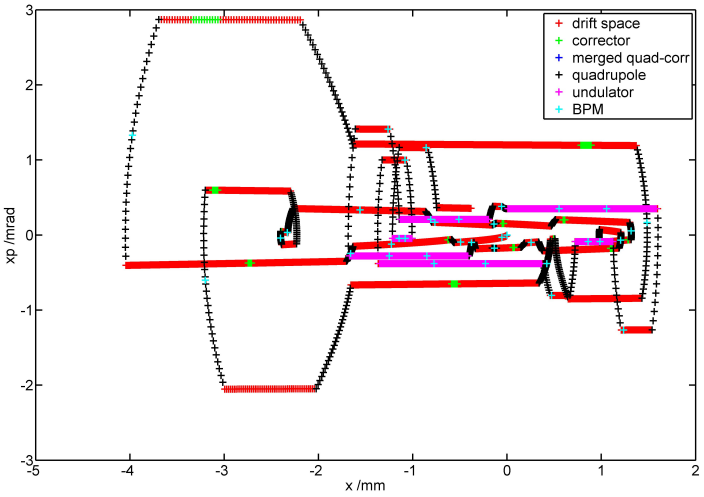

Figure D.1.: x - x' phase space for the initial trajectory.

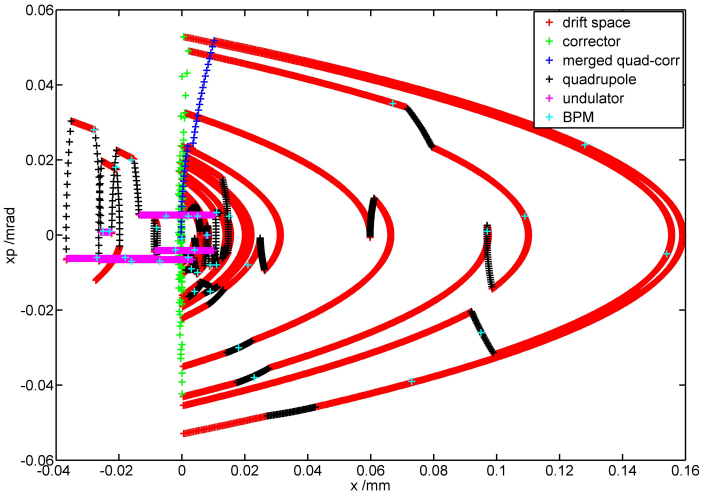

Figure D.2.: x - x' phase space for the trajectory with applied compensation (method $f = \infty$) for the Earth's magnetic field.